Marine Pollution Bulletin 171 (2021) 112917

Contents lists available at ScienceDirect

Marine Pollution Bulletin

journal homepage: www.elsevier.com/locate/marpolbul

MV *Wakashio* grounding incident in Mauritius 2020: The world's first major spillage of Very Low Sulfur Fuel Oil

Alan G. Scarlett [a,*], Robert K. Nelson [b], Marthe Monique Gagnon [c], Alex I. Holman [a], Christopher M. Reddy [b], Paul A. Sutton [d], Kliti Grice [a,*]

[a] Western Australian Isotope and Geochemistry Centre, School of Earth and Planetary Sciences, Curtin University, Perth, Western Australia 6102, Australia
[b] Department of Marine Chemistry and Geochemistry, Woods Hole Oceanographic Institution, Massachusetts, MA 02543, USA
[c] School of Molecular and Life Sciences, Curtin University, Perth, Western Australia 6102, Australia
[d] Biogeochemistry Research Centre, School of Geography Earth & Environmental Sciences, University of Plymouth, Plymouth, England, UK

ARTICLE INFO

Keywords:
Mauritius oil spill
VLSFO
Fuel oil
GC × GC
Stable isotopes
High-resolution mass spectrometry

ABSTRACT

Very Low Sulfur Fuel Oils (VSLFO, <0.5% S) are a new class of marine fuel oils, introduced to meet recent International Maritime Organization regulations. The MV *Wakashio* was reported to have released 1000 t of VLSFO when it grounded on a reef in Mauritius on 25th July 2020. A field sample of oily residue contaminating the Mauritian coast was collected on 16th August 2020 and compared with the *Wakashio* fuel oil. Both oils were analyzed for organic and elemental content, and stable isotope ratios $\delta^{13}C$ and $\delta^{2}H$ measured. Comprehensive two-dimensional gas chromatography with high-resolution mass spectrometry was used to identify and compare biomarkers resistant to weathering. The aromatic content in the VLSFO was relatively low suggesting that the potential for ecosystem harm arising from exposure to toxic components may be less than with traditional fuel oil spills. The *Wakashio* oil spill is, to our knowledge, the first documented spill involving VLSFO.

1. Introduction

In an attempt to reduce the worldwide emissions of sulfur oxides (SOx) to the atmosphere with the aim of providing major human health and environmental benefits, a new Global Sulfur Cap regulation was implemented (IMO/MARPOL convention, Annex VI) from January 2020 (IMO, 2020). Previously, ships could burn marine fuels with sulfur contents of up to 3.5% but now reduced to ≤0.5% S (IMO, 2020). The compliant residual fuels, termed "Very Low Sulfur Fuel Oil" (VLSFO), are replacing the traditional intermediate fuel oils or heavy fuel oils e.g. IFO 180 and IFO 380 but little is known about the characteristics of VLSFOs other than a tendency to possess high pour points (Sørheim et al., 2020). Having some understanding about the character and behavior of VLSFO is critical to planning, responding, clean-up, and determining the extent of damages and recovery of accidental releases (Hook et al., 2016).

Although there is likely to be considerable variation in the characteristics of VLSFO due to differences in feedstock, refinery type, and conversion processes used to reduce the S content e.g. catalytic cracking and hydrodesulfurization (Sørheim et al., 2020), there is a need to take every opportunity to increase our understanding of the fate and behavior of these oils. Such an opportunity arose when the bulk carrier MV *Wakashio* ran aground on a coral reef offshore of Pointe d'Esny, Southeast Mauritius, on 25th July 2020 while traveling to Brazil from China (Lewis, 2020). The area is a recognized wildlife sanctuary and includes sites of international importance identified in the Ramsar Convention on Wetlands (Ramsar, 2020). Within a fortnight, the cracked hull began leaking oil into the ocean. The vessel eventually broke in two by 15th August 2020; an estimated 1000 metric tonnes (260,000 US gallons) of fuel oil leaked into the Indian Ocean (Lewis, 2020; Mitsui-O.S.K.Lines, 2020). At the time the vessel ran aground there were approximately 3800 t of VLSFO, 200 t of diesel oil, 100 t of lubricant oil and residual oil on board (Mitsui-O.S.K.Lines, 2020). Satellite imagery showed thick oil contamination along the coast had occurred by 6th August 2020 (Rajendran et al., 2021). The lack of any independent analysis of the spilled oil has led to confusion and speculation in the media which is unlikely to be helpful to the people of Mauritius whose economy is largely reliant on tourism and fishing. Following the *Deepwater Horizon* spill in 2010, tourism and fishing were not only impacted directly by the spilled oil but also by people's perception (Nelson et al.,

* Corresponding authors.
E-mail addresses: alan.scarlett@curtin.edu.au (A.G. Scarlett), k.grice@curtin.edu.au (K. Grice).

https://doi.org/10.1016/j.marpolbul.2021.112917
Received 15 July 2021; Received in revised form 24 August 2021; Accepted 26 August 2021
Available online 3 September 2021

2018). Consequently, it is important to confirm that it was VLSFO from the *Wakashio* that contaminated the Mauritius coast and to investigate the characteristics of both the fuel oil and spilled oil so that informed decisions can be made regarding post-spill management strategies.

While spills of fuel oils occur more frequently than crude oils and have been well studied (e.g. Chen et al., 2018; Fingas, 2016; Lemkau et al., 2010; Nelson et al., 2006), the varying hydrocarbon composition, spill location, and other factors has led to a wide range of short- and long-term fates and impacts for each event. For example, field studies immediately after the Bouchard 120 (Buzzards Bay, MA in 2003, (Nelson et al., 2006)) and Cosco Busan (San Francisco Bay in 2007, (Lemkau et al., 2010)) spills revealed that polycyclic aromatic hydrocarbons (PAHs) partitioned into the surrounding water and the air differently. Approximately equal amounts of naphthalene were lost to the water and air following the Bouchard 120 while loss to air (evaporation) was much more dominant after the Cosco Busan. A critical aspect of the scientific evidence for assessing the impact of a spill is the ability to link weathered oil products found in the environment with that of the suspected spilled oil. Early characterization of spilled oil is therefore an important step in the mitigation of oil spills, as well as for litigation and monitoring of ecosystem recovery (Hook et al., 2016). To date, no information concerning the fate of the fuel oil released following the grounding of *Wakashio* has been published. If the spillage from the *Wakashio* was VLSFO, this will be the first documented major spill of its kind since the introduction of the new IMO regulations.

The main aims of this research were to characterize the fuel oil from the *Wakashio* and to compare this to an oily residue collected following the grounding of the ship, thus enabling confirmation that the oil released was VLSFO. The research will also provide insight into the weathering characteristics of this VLSFO and inform on its potential effect upon the environment. Multi-chromatographic and spectroscopic techniques were performed that would indicate components of the fuel oil lost to the atmosphere and to the water-column whereupon they can become bioavailable and cause adverse effects in organisms, and those more resistant to weathering that could be used for forensic identification and comparison in the future. Conventional gas chromatography–mass spectrometry (GC–MS) plus high temperature GC (HTGC) were used to characterize the oils. Comprehensive two-dimensional gas chromatography with flame ionization detection (GC × GC-FID) and with high-resolution mass spectrometry (GC × GC-HRT), has been shown to be highly capable of resolving complex mixtures such as weathered crude oils (Nelson et al., 2019) and has been employed in this investigation. The oils were also subject to compound specific isotope analysis (CSIA) by gas chromatography isotope-ratio mass spectrometry (GC-irMS). Elemental analyses by inductively coupled plasma-mass spectrometry (ICP-MS) provided further insight into the nature of the oils.

2. Materials and methods

2.1. Wakashio fuel oil and collection and transportation of field sample spilled oil

Fuel oil from the *Wakashio* was supplied by SINTEF, Norway. The field oil sample was collected from offshore floating residues (20°23′49.7″S, 57°41′58.3″E) on 16th August 2020 by a volunteer worker. Significant quantities of oil have been documented as present in this area from 6th August (Rajendran et al., 2021). The collection site was four nautical miles (NM), ~7,5 km, northwest of where the *Wakashio* grounded. The sample was kept cool until shipment to Curtin University, Australia. Upon arrival the sample was divided into aliquots. Aliquots of the Mauritius oil and the *Wakashio* fuel oil were sent to Woods Hole Oceanographic Institution (WHOI) for GC × GC-HRT and to Plymouth University for HTGC. The oils were retained at Curtin University for analyses by GC–MS, GC-irMS and ICP-MS. Chromatograms and key biomarker ratios of the aliquots were compared between laboratories to check for any losses during transport.

2.2. ICP-MS

The samples were weighed and repeatedly digested in nitric acid, and finally in a mixture of nitric/perchloric acids. The digestate was taken to incipient dryness and the residue was dissolved in high purity nitric (0.7 mL), hydrochloric (0.2 mL) acids and high purity water (25 mL). This solution was then suitably diluted for ICP-AES and ICP-MS analysis. Concentrations were determined using AccuTrace High Purity multi-element standards (Choice Analytical, Thornleigh NSW, Australia).

2.3. GC–MS

Prior to GC–MS analyses, the oils were spiked with perdeuterated standards tetralin-d_{12}, naphthalene-d_8 and phenanthrene-d_{10} (Sigma-Aldrich Pty. Ltd., Sydney, Australia). They were then separated by silica gel chromatography into saturate (100% *n*-hexane), aromatic (7:3 *n*-hexane: dichloromethane (CH_2Cl_2)), polar (1:1 CH_2Cl_2:methanol), and highly polar (100% methanol) fractions. GC–MS analyses were performed using a HP-6890A gas chromatograph (Agilent, Santa Clara, CA, USA) interfaced to a HP-5973 mass selective detector (Agilent). Analyses of the saturated hydrocarbon fractions were performed using a DB-1 ms capillary column and the aromatic fraction using a DB-5 ms (both 60 m × 0.25 mm internal diameter × 0.25 μm film thickness). For the saturates fraction, the GC oven was programmed from 40 °C (held 2 min) to 320 °C at 6 °C min^{-1} with a final hold time of 26 min. For the aromatics fraction, the GC oven was programmed from 40 °C (held 1 min) to 325 °C at 3 °C min^{-1} with a final hold time of 30 min. Ultra-high purity helium was used as the carrier gas with a constant flow of 1 mL min^{-1}. Sample injection was 1 μL pulsed splitless at 280 °C. The MSD was operated at 70 eV with a source temperature of 230 °C. Mass spectra were acquired in full scan mode. Identification and quantification of PAHs was by reference to certified analytical standards (Neochema, Bodenheim, Germany) and corrected for losses using internal standards.

2.4. HTGC

High temperature GC-FID was utilized to detect high-molecular-weight components not observed with normal range GC. A 0.5 μL sample aliquot was 'hot' (sample and syringe pre-heated at 70 °C) manually injected via a cool-on-column inlet (track oven mode; +3 °C) onto a Vf-5ht Ultimetal column (15 m × 0.25 mm × 0.1 μm; Agilent Technologies Limited, UK) operated with He carrier gas (constant flow mode; 1 mL min^{-1}) and the GC oven (HP6890) programmed from 40 to 430 °C at 10 °C min^{-1} with 10 min isothermal hold. The FID high temperature jet was operated at 430 °C (FID gas flows optimized at H_2 40 mL min^{-1}, air 450 mL min^{-1} and N_2 make-up 45 mL min^{-1}).

2.5. GC×GC-FID

Analyses were performed on a LECO instrument consisting of an Agilent 7890A GC configured with a split/splitless auto-injector (7683B series) and a dual stage cryogenic modulator (LECO, Saint Joseph, Michigan). The GC × GC-FID carrier gas was hydrogen (H_2) at a flow rate of 1 mL min^{-1} and the instrument was operated in constant flow rate mode. Samples were injected in splitless mode. Samples were prepared at a concentration of 5 mg mL^{-1} neat fuel in CH_2Cl_2. The cold jet gas was dry N_2 chilled with liquid N_2. The hot jet temperature offset was 5 °C above the temperature of the secondary GC oven and the inlet temperature was isothermal at 310 °C. Two capillary GC columns were utilized for these GC × GC analyses. The first-dimension column was a Restek Rxi-1 ms, (60 m length × 0.25 mm × 0.25 μm) and second-dimension separations were performed on a 50% phenyl polysilphenylene-siloxane column (SGE BPX50, 1.2 m × 0.10 mm × 0.1

μm). The temperature program of the main oven was held isothermal at 65 °C (12.5 min) and was then ramped from 65 to 340 °C at 1.25 °C min^{-1}. The second-dimension oven was held isothermal at 70 °C (12.5 min) and then ramped from 70 to 345 °C at 1.25 °C min^{-1}. The hot jet pulse width was 1 s, and the modulation period between stages was 6.5 s and a cooling period of 2.25 s between stages. FID data was sampled at an acquisition rate of 100 data points s^{-1}.

2.6. GC×GC-HRT

High resolution analyses by GC × GC-HRT utilized a LECO Pegasus GC × GC-HRT 4D instrument consisting of an Agilent 7890B GC configured with a LECO LPAL3 split/splitless auto-injector and a dual stage cryogenic modulator (LECO, Saint Joseph, Michigan). The carrier gas was He at a flow rate of 1 mL min^{-1} in constant flow mode. Samples were prepared at a concentration of 5 mg mL^{-1} neat fuel in CH_2Cl_2 and were injected in splitless mode. The cold jet gas was dry N_2 chilled with liquid N_2. The hot jet temperature offset was 15 °C above the secondary oven and the inlet temperature was isothermal at 310 °C. The first-dimension column was a Restek Rxi-1 ms, (60 m × 0.25 mm × 0.25 μm) and second-dimension separations were performed on a 50% phenyl polysilphenylene-siloxane column (SGE BPX50, 1.2 m × 0.10 mm × 0.1 μm). The temperature program of the main oven was held isothermal at 80 °C (12.5 min) and was then ramped to 330 °C at 1.25 °C min^{-1}. The second-dimension oven was held isothermal at 85 °C (12.5 min) and then ramped from 85 to 345 °C at 1.25 °C min^{-1}. The hot jet pulse width was 2 s, and the modulation period between stages was 8 s with a cooling period of 2 s between stages. HRT data was sampled at an acquisition rate of 200 spectra s^{-1}. The ionization method was electron ionization (EI) with an electron energy of −70 eV and an extraction frequency of 1.5 kHz.

2.7. GC-irMS

Saturate fractions were obtained as for GC–MS but without the addition of perdeuterated standards. $\delta^{13}C$ and $\delta^{2}H$ of *n*-alkanes and isoprenoids pristane and phytane was performed using a Thermo Delta V Advantage irMS, coupled to a Thermo Trace GC Ultra via a GC Isolink and Conflo IV. The irMS measured fragment ions *m/z* 44, 45 and 46 for CO_2 or *m/z* 2 and 3 for H_2. The $\delta^{13}C$ and $\delta^{2}H$ values were calculated from the measured masses by Thermo Isodat software. Values were converted to the VPDB / VSMOW scales by comparison with an in-house mixture of *n*-alkane standards (*n*-C_{11}, *n*-C_{13}, *n*-C_{14}, *n*-C_{17}, *n*-C_{18}, *n*-C_{19} and *n*-C_{25}) of known isotopic composition ($\delta^{13}C$ from −25.3 to −32.2‰, $\delta^{2}H$ from −104.2 to −268.6‰), and commercially available isotopic standards from Indiana University (http://pages.iu.edu/~aschimme/hc.html): *n*-C_{22} ($\delta^{13}C$ -32.87 ± 0.03‰, $\delta^{2}H$ -62.8 ± 1.6‰) and squalane ($\delta^{13}C$ -20.49 ± 0.02‰ and $\delta^{2}H$ -168.9 ± 1.9‰). Samples were measured in triplicate, and standard errors were less than 0.5‰ for $\delta^{13}C$ and 5‰ for $\delta^{2}H$.

3. Results and discussion

3.1. General characterization

Elemental analysis revealed the S content of both the *Wakashio* fuel oil and the field sample was <0.5% (Table 1) consistent with a VLSFO. A one-dimensional (1D) total ion chromatogram (TIC) comparison of the saturate fractions of the oils revealed a distinct decreased relative abundance of low molecular components consistent with weathering in the field sample but otherwise the oils appeared similar (Fig. 1). Extracted ion fragmentograms by GC–MS for key biomarkers (Fig. 1) indicated the field sample was derived from the *Wakashio* fuel oil but were present in low abundances in both oils. Extracted ion fragmentograms by GC–MS for parent and alkylated naphthalenes, phenanthrenes and dibenzothiophenes within the aromatic fractions of the oils also indicated a common origin although some differences were evident

Table 1
Mean (standard deviation, $n = 3$) concentrations (μg g^{-1}) of major elements in *Wakashio* fuel oil and a field sample of spilled oil as determined by inductively coupled plasma-mass spectrometry. Ratios of V/(V + Ni) also provided.

	S	Na	Ca	Mg	K	Fe	Al	Ti	P	V	Ni	Sr	Si	Mn	Ba	Cr	Cu	Zn	V/(V + Ni)
Fuel oil	3347	110	16	11.4	<1	15.2	<7.4	<0.5	<12	7.5	3.4	0.2	< 4.1	0.3	4.9	< 0.02	0.3	4.3	0.69
	(637)	(2.5)	(1.3)	(0.5)		(2.4)				(0.8)	(0.2)	0.0		(0.1)	(0.1)		(0.1)	(2.6)	(0.02)
Spill oil	2137	3697	626	602	232	207	131	21	14	3.2	2.7	6.0	5.7	3.4	0.4	0.7	0.7	0.8	0.55
	(207)	(99)	(130)	(6)	(14)	(19)	(14)	(1.9)	(1.2)	(0.2)	(0.4)	(0.8)	(6.6)	(1.1)	(0.1)	(0.4)	(0.3)	(0.3)	(0.02)

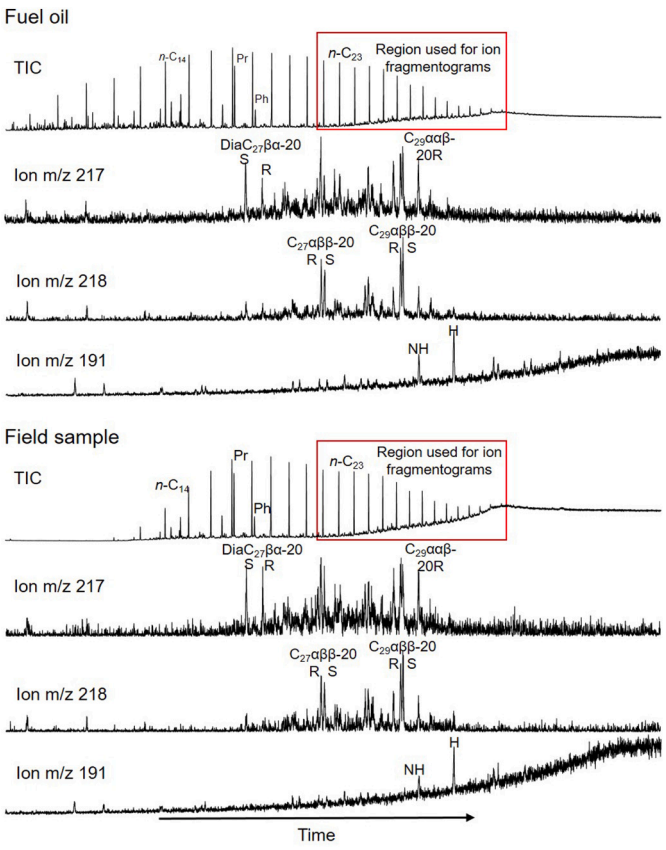

Fig. 1. GC–MS total ion chromatograms (TIC) for saturate fractions of *Wakashio* fuel oil (top panel) and a field sample (bottom panel). Box shows biomarker region used for ion fragmentograms for diasteranes/steranes (*m/z* 217 and 218) and terpane hopanoids (m/z 191). A key to compound name abbreviations is provided in Appendix A.

(Fig. 2). Further analysis by GC × GC-FID of the whole fuel oil, i.e. without any procedural work-up that can result in losses, from the *Wakashio* fuel oil showed it to be mostly comprised of straight chain and branched alkanes with lesser quantities of multicyclic saturated, aromatic, and heterocyclic compounds (Fig. 3A). The aromatic and heterocyclic content was unusually low compared with typical marine fuel oils (Uhler et al., 2016). In the following sections, detailed characterisations are presented on the fuel oil and field sample of spilled oil collected on August 16th 2020.

3.2. Elemental analysis by ICP-MS

The sulfur content of the *Wakashio* fuel oil was 0.33% (SD = 0.06%, $n = 3$) and similar to the field sample ~ 0.21% (SD = 0.02%, $n = 3$), well within the limit for VLSFO of 0.5% (Table 1). One difference in the fuel oil and field sample was the entrainment of seawater in the field samples based on the presence of some of the major ions of seawater (e.g., sodium and calcium). Hence, as seawater is contributing to the mass of the spilled oil, the absolute concentrations of elements will be underestimated somewhat when compared with the unweathered fuel oil. Vanadium (V) and nickel (Ni) are abundant metals within crude oils associated with porphyrin complexes (Barwise, 1990). Both the absolute and relative concentrations of V and Ni have been used to classify crude oils and provide information on their source (Barwise, 1990). Concentrations of V and Ni were very low (<10 μg g^{-1}) in both the fuel and spilled oils (Table 1). The ratio of V/(V + Ni) was 0.69 for the fuel oil compared to 0.55 in the spilled oil (Table 1). Elemental analysis appears to have the potential to discriminate fuel oils if, for example, much higher concentrations of V and/or Ni were present. However, weathering effects, especially the formation of emulsions, need to be taken into consideration. Elemental data for other Low Sulfur Fuel Oils (LSFOs) are not yet available for comparison.

3.3. HTGC

Heavy fuel oils (HFOs) contain high molecular weight components including *n*-alkanes and waxes, many of which are outside the normal range for GC analysis (Uhler et al., 2016) and, as such, may therefore not be apparent in Fig. 1. However, these components could account for the high pour points observed in LSFOs generally (Sørheim et al., 2020). Although the *Wakashio* fuel oil *n*-alkane range extended up to *n*-C_{57}, determined using the HTGC method herein, the relative abundances of >*n*-C_{40} hydrocarbons were very low (Fig. S1). The HTGC profile of spilled oil matched that of the fuel oil from around *n*-C_{20} and higher, although the chromatographic areas were lower for the former. As the oils were analyzed at the same injection concentration, this likely reflects that some components from the weathering of the spilled oil were not amenable to GC. The formation of water-in-oil emulsion would account for this.

3.4. Biomarker ratios and profiles by GC×GC-FID and GC×GC-HRT

Conventional 1D chromatograms of compound classes acquired by selected *m/z* ions, and the corresponding mass spectra from individual 1D GC peaks, can be affected by matrix effects and interferences, especially co-eluting peaks; this is particularly an issue in the biomarker elution region. The use of GC × GC is one method that overcomes such problems, producing more selective chromatograms with higher peak capacities than one dimensional chromatography (Eiserbeck et al., 2012; Grice and Eiserbeck, 2014). High resolution mass spectrometry provides additional separation power capable of resolving peaks with the same retention time and same nominal mass (Nelson et al., 2019). For the methodology employed for this study, the 2D chromatograms show separation by volatility along the 1st dimension (*x*-axis) and by polarity on the 2nd dimension (*y*-axis). The chromatograms are either displayed as 3D 'surface plots' where peaks rise with increasing intensity or in 'plan view' where the color transition from blue to red is used to indicate relative intensity.

Biomarkers are molecules in petroleum derived from once-living plants and animals (Peters et al., 2005). Due to their resistance to biodegradation, biomarkers are useful for characterizing petroleum contamination in the environment (Wang et al., 2016). Although in relatively low abundance, suites of hopanoid biomarkers were identified in both the fuel (Fig. S2) and the spilled oils using the enhanced peak capacity and MS resolving power of GC × GC-HRT and the biomarker profiles showed remarkable similarity (Fig. 4). A comparison of key hopanoid biomarker ratios (Table 2) were near identical providing strong evidence that the field oil sample collected four NM from the ship was indeed the spilled fuel oil and not one of the other oils on board the *Wakashio* or derived from a separate source. Similarly, profiles of steranes and diasteranes biomarkers were near identical (Fig. S3). The improvement in resolution achieved using exact mass rather than traditional whole unit mass spectrometry was apparent for the hopanoids (Fig. S2) and for the steranes and diasteranes (Fig. S4). The use of GC × GC-HRT provides unambiguous identification of biomarkers (mass accuracies typically <1 ppm) even in highly weathered oils. The ratios of various biomarkers thus provide a unique fingerprint of the spilled oil which can be used to compare with oil from the fuel tank of *Wakashio* and any future contamination of the Mauritius shore and organisms.

Marine fuel oils are normally rich in organic sulfur compounds such as the dibenzothiophenes (DBTs) (Uhler et al., 2016). Although in very low abundances in both the fuel and spilled oil, some were present that could provide diagnostic evidence. Dibenzothiophene and its alkylated homologs showed the same profile in both oils (Fig. 5). Abundances decreased with increasing alkylation suggesting that weathering had

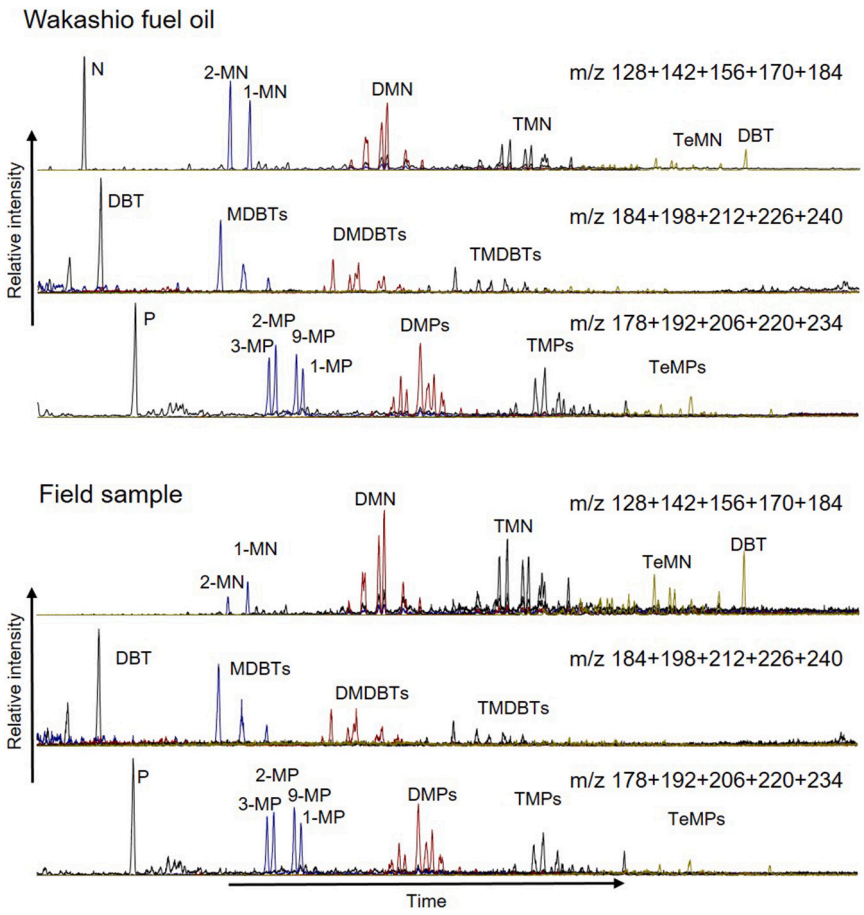

Fig. 2. GC–MS extracted ion fragmentograms for major parent and alkylated homolog series of aromatic compounds, $C_{0–4}$ naphthalenes, $C_{0–4}$ dibenzothiophenes (DBTs), and $C_{0–4}$ phenanthrenes within *Wakashio* fuel oil (top panel) and a field sample (bottom panel). The DBTs and phenanthrenes are on the same time scale. The naphthalenes elute earlier in the chromatogram. N = naphthalene, P = phenanthrene, M = methyl, DM = dimethyl, TM – trimethyl and TeM = tetramethyl.

little effect on these compounds. Exact mass resolution of the DBT homologs in 1D chromatograms are available in Fig. S5. Phenanthrothiophenes possess an additional ring with extra two carbons and are therefore even less susceptible to evaporative or dissolution processes. Present in extremely low abundances, the profiles of the oils matched with greater abundances of C_3- and $C_{4–}$ phenanthrothiophenes (Fig. S6). Benzonaphthothiophenes, containing a further two carbons, were also detectable but again at very low abundance and with similar profiles for both fuel and spilled oils (Fig. S7). Exact mass resolution of the benzonaphthothiophene homologs in 1D chromatograms are available in Fig. S8. Profiles of these sulfur-heterocyclics could potentially prove to be diagnostic of differences in the methods used to lower the sulfur content in fuel oils, and hence warrant further investigation using other LSFOs.

Profiles of additional heterocyclics containing oxygen and nitrogen were also examined. In the *Wakashio* fuel oil, acenaphthenones/dibenzofurans showed decreasing abundances with increasing alkylation but the parent and methyl structures were less abundant in the spilled oil consistent with light weathering (Fig. S9). Carbazoles and benzocarbazoles were in negligible amounts in both oils. This raises the question as to whether these nitrogen-containing compounds are also removed during the sulfur removal process whereas those containing oxygen are less affected. Further studies with multiple LSFOs are necessary to explore whether this is specific to a particular process or whether it merely reflects the composition of the feedstock used in the fuel oil.

3.5. *Quantification of aromatic components and assessment of evaporative losses and dissolution*

Having verified that the field sample of oily residue was indeed derived from VLSFO spilled from the *Wakashio*, it may be useful to understand the quantity of potentially toxic compounds that was released into the environment. The aromatic fraction of the *Wakashio* fuel oil was dominated by monoaromatic hydrocarbons (MAH), mainly low weight alkylbenzenes up to 148 Da plus tetrahydronaphthalenes (tetralins, also indanes) up to 174 Da (Figs. 3C and 6). The former was found to be absent in the spilled oil and the latter was much reduced. From the 1000 t discharged to the ocean, an estimated 5.3 g of MAH kg^{-1} fuel oil was lost in the time between when the spill commenced and the field sample was collected (Fig. 6), probably due mainly to evaporative processes. Naphthalene was present at low concentration (~0.5 g kg^{-1}) in the fuel oil but was absent in the spilled oil. Alkylated naphthalenes were much lower in the spilled oil until equivalence was reached at the C_4 homolog (Fig. 6). Around 5.4 g $C_{0–3}$ naphthalenes (parent and C1 to C3 alkyl homologs) kg^{-1} fuel oil were lost prior to sampling but some of this likely entered the water column rather than evaporated. Even in the unweathered fuel oil, the naphthalenes and phenanthrenes were considerably lower than in typical heavy fuel oils (Uhler et al., 2016). In fact, the PAHs in the *Wakashio* fuel oil were generally much lower than in the majority of the 71 fuel oils reported by Uhler et al. (2016). The PAH content of two VLSFO was recently reported (Sørheim et al., 2020) to be low as was an ultra-low sulfur fuel oil (ULSFO, defined as <0.1% S). It is possible that the phenomena of low aromatic content may be typical of LSFO generally rather than this particular fuel oil, and is

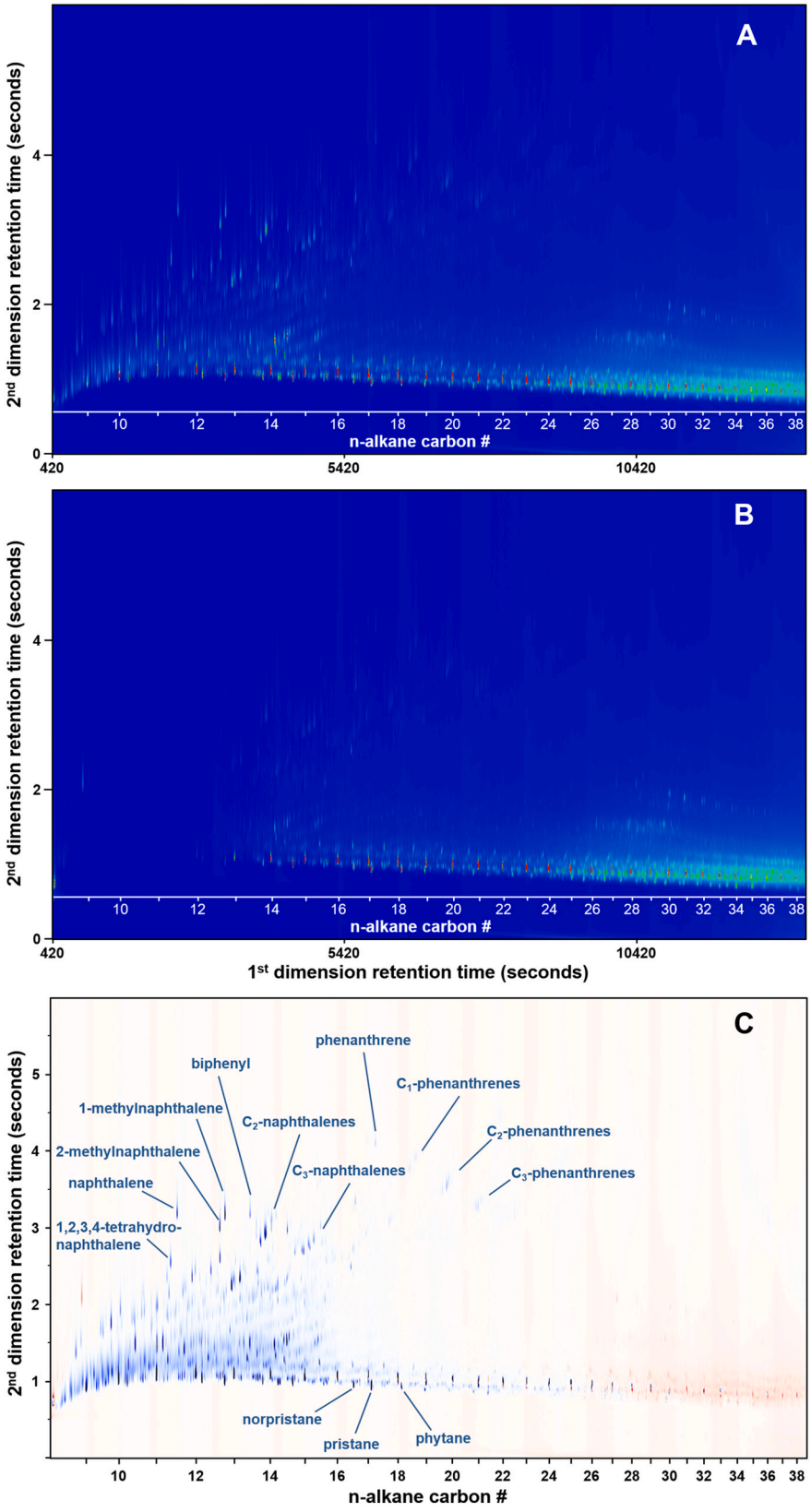

Fig. 3. Two-dimensional gas chromatograms of (A) *Wakashio* fuel oil and (B) a field sample of spilled oil. Peak intensity increases from blue to red. Panel C shows a difference chromatogram in which compounds that are more abundant in the *Wakashio* fuel oil appear blue and those more abundant in the spilled oil appear red. Those that vanish are the same relative abundance in both oils. (For interpretation of the references to color in this figure legend, the reader is referred to the web version of this article.)

probably related to the catalytic hydrogenation sulfur removal process. The S-containing heterocyclic dibenzothiophene (DBT) and its alkylated homologs were also in very low abundance (<0.5 g kg^{-1}, Fig. 6) consistent with that reported for both VLSFO and ULSFO (Sørheim et al., 2020). The potential for toxic activity arising from the aromatic hydrocarbons present in the *Wakashio* fuel oil and those released into the environment following the spill in Mauritius is discussed below.

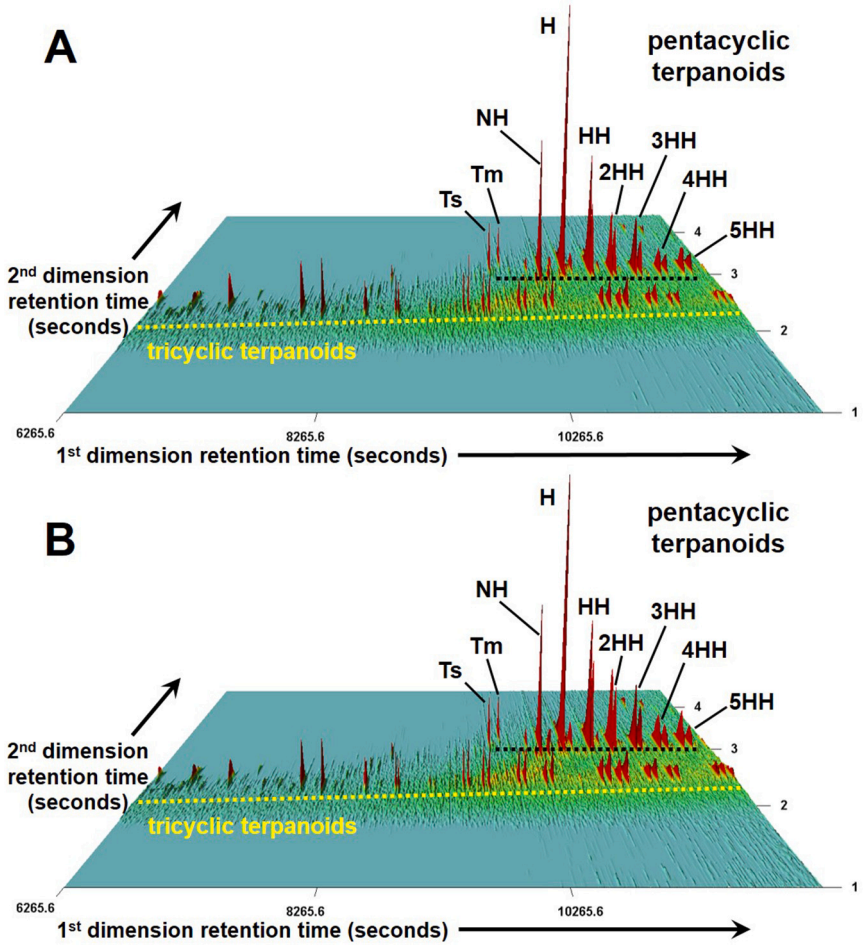

Fig. 4. GC × GC-HRT surface plots of extracted ion chromatograms for *m/z* 191.179 comparing terpane biomarkers present in (A) *Wakashio* fuel oil and (B) a field sample of spilled oil. A key to compound name abbreviations is provided in Appendix A.

Table 2
Comparison of key biomarker ratios derived from GC × GC-FID analyses of *Wakashio* fuel oil and a field sample of spilled oil.

Ratio	*Wakashio* fuel oil	Spilled oil
Ts/Tm	1.57	1.56
Ts/(Ts + Tm)	0.61	0.61
Ts/H	0.30	0.29
Tm/H	0.19	0.18
BNH/H	0.1	0.1
C29-Ts/H	0.22	0.22
NM/H	0.04	0.05
M/H	0.04	0.04
HH(S)/H	0.49	0.49
HH(R)/H	0.37	0.36
G/H	0.02	0.02
2HH(S)/H	0.37	0.36
2HH(R)/H	0.25	0.25
3HH(S)/H	0.25	0.25
3HH(R)/H	0.15	0.14
4HH(S)/H	0.19	0.18
4HH(R)/H	0.10	0.09
5HH(S)/H	0.19	0.19
5HH(R)/H	0.11	0.11

Abbreviations defined in Appendix A.

3.6. Isotopic analysis by GC-irMS

Short-term weathering experiments have shown that effects on $\delta^{13}C$ values of individual *n*-alkanes (>C11) were not significant so the stable carbon isotope profile can be a useful tool for tracing the source of an oil spill (Asif et al., 2011; Li et al., 2009). Although both oil samples showed a general trend of increasingly negative $\delta^{13}C$ values with increasing carbon number, $\delta^{13}C$ ratio values of the *n*-alkanes >*n*-C_{20} in the *Wakashio* fuel oil were appreciably more depleted than the field sample consistent with evaporative losses of the lighter isotope due to weathering (Fig. 7A). Peak areas for low-molecular-weight alkanes in the spilled oil were relatively low, reflecting major evaporative losses, which could have led to greater co-elution with minor branched and cyclic alkanes which affected $\delta^{13}C$ values. The isoprenoids pristane and phytane had similar values to that of the corresponding *n*-alkanes, although pristane had somewhat more negative $\delta^{13}C$ values in the fuel oil. There was however an offset between isoprenoids and *n*-alkane $\delta^{2}H$ values (−10‰ and − 13‰) for pristane and phytane respectively in the spilled oil (Fig. 5B). This relatively small offset may indicate significant hydrogen exchange (^{2}H enrichment) has occurred and would normally suggest a more mature source feed oil (Asif et al., 2011; Dawson et al., 2005) but typical fuel oils are generally derived from multiple feed oils. Isotopic data for other LSFOs are not yet available for comparison.

3.7. Potential environmental impact

There has been considerable speculation about the possible effects of the *Wakashio* oil spill with deaths of wildlife, including dolphins, attributed to the spill e.g. https://www.bbc.com/news/world-africa-53917793 (accessed 12th July 2021). The uncertainty about what was actually spilled and the nature of VLSFO has added to this concern and confusion. Based on the characterization of the oils, some initial

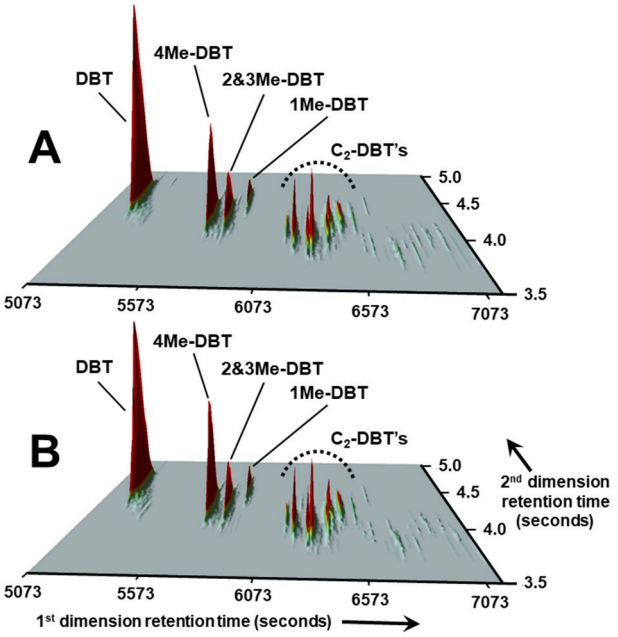

Fig. 5. GC × GC-HRT surface plots comparing dibenzothiophenes (DBT) present in (A) *Wakashio* fuel oil and (B) a field sample of spilled oil using positive ion monoisotopic masses *m/z* 184.0341 (DBT), *m/z* 198.0498 (C_1-DBT's), *m/z* 212.0654 (C_2-DBT's), *m/z* 226.0811 (C_3-DBT's), *m/z* 240.0967 (C_4-DBT's) and *m/z* 254.1124 (C_5-DBT's).

assessment of the potential for toxicity can be discussed.

The unusually small aromatic fraction and corresponding low PAH content of the spilled oil (Figs. 2 and 5) would suggest that this oil is potentially less toxic relative to a conventional HFO or many crude oils. PAHs that have a toxic mode of action mediated via the aryl hydrocarbon receptor (AhR) (Shimizu et al., 2000) e.g. benzo[*a*]pyrene and chrysene, were found to be in extremely low concentrations in the low sulfur oils (Figs. 3 and 6). Alkylated homologs of lower molecular weight three-ring PAHs have been associated with toxic effects in fish, e.g. key developmental defects were found to be induced by weathered crude oil exposure mediated by alkylphenanthrenes through AhR-independent disruption of cardiovascular function and morphogenesis (Incardona et al., 2005). The difference between the phenanthrene concentration in the fuel oil and that of the field oil sample was ~100 mg kg^{-1} oil and around 500 mg kg^{-1} oil for the $C_{1–4}$ alkylphenanthrenes (Fig. 6). Hence, of the reported 1000 t of fuel oil spilled, approximately 0.5 t of alkylphenanthrenes would have entered the environment. The most abundant PAHs in the fuel oil were alkylnaphthalenes (Figs. 2, 3 and 6). All of the parent compound and about 5400 mg kg^{-1} oil of $C_{1–4}$ alkylnaphthalenes were lost to weathering i.e. about 6 t in total entered the environment. Low molecular weight alkylnaphthalenes are highly soluble in water but also subject to evaporation so are rapidly lost especially in warm waters (NRC, 2003). Increasing alkylation reduces volatility and solubility but can result in increased bioaccumulation by organisms, especially those with very limited ability to metabolize hydrocarbons such as marine mollusks (Booth et al., 2007). Quantitative Structure Activity Relationship models for mussel clearance rates have shown amplified toxicity with increasing molecular weight of naphthalenes (Donkin et al., 1991) although molecular structure is also an important influence (Scarlett et al., 2011). The relatively large component of low-molecular-weight MAH in the fuel oil (compared to PAH), much reduced in the spilled oil, should also be considered. Due to their high volatility, many of these MAH would have evaporated. The alkylated tetralins and indanes could have dissolved and added to the acute toxicity in the shallow coastal waters. Branched alkylated MAH have been reported to accumulate in bivalve mollusks resulting in reduced filtration rates via narcosis toxicity (Booth et al., 2008; Booth et al., 2007). Trophic transfer of MAH and subsequent effects on the predator species have also been demonstrated (Scarlett et al., 2009). Although in relatively low concentrations, higher weight alkylated MAH were present in both the fuel and spilled oil (Fig. 3). The difference chromatogram (Fig. 3C) shows that the higher weight MAH were still present in the spilled oil and therefore likely to continue to slowly release into the ocean in the future. Consequently, future sampling of organisms from the Mauritius coastline and reefs should include quantification of this class of compounds in addition to the usual PAHs.

In total, about 13 t of aromatic compounds are estimated to have been lost from the 1000 t of fuel oil spilled (Fig. 6), some of which would have entered the water column. The shallow coastal waters, lagoons and reef systems in the vicinity of the spilled oil would likely have prevented

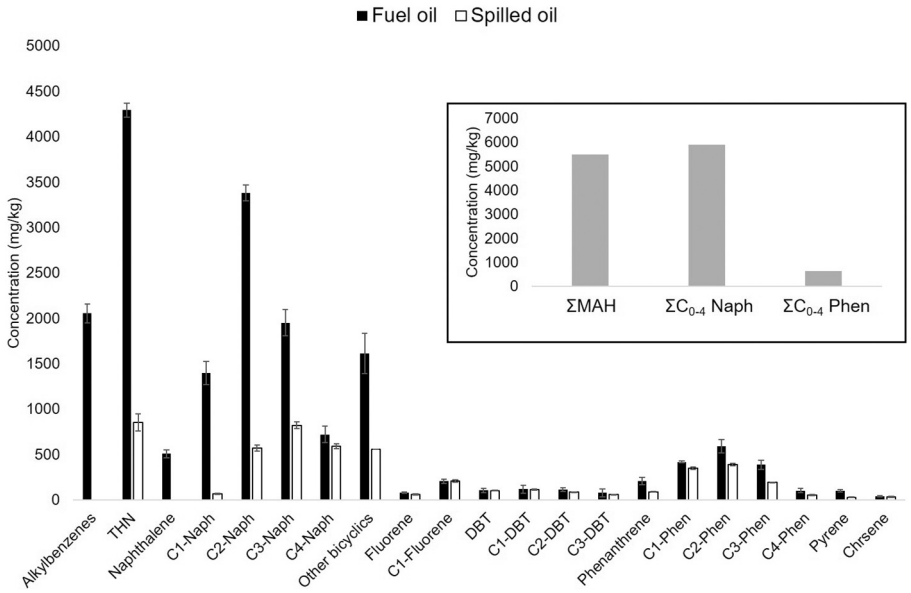

Fig. 6. Mean concentrations of monoaromatic and polycyclic aromatic hydrocarbons present in Wakashio fuel oil (black bars) and spilled oil (white bars). Only low weight alkylbenzenes up to 148 Da and tetrahydronaphthalenes (THN, includes tetralins and indanes) up to 174 Da were quantified. Error bars are one standard deviation, $n = 3$. Insert shows differences in concentrations between the fuel and spilled oils (grey bars).

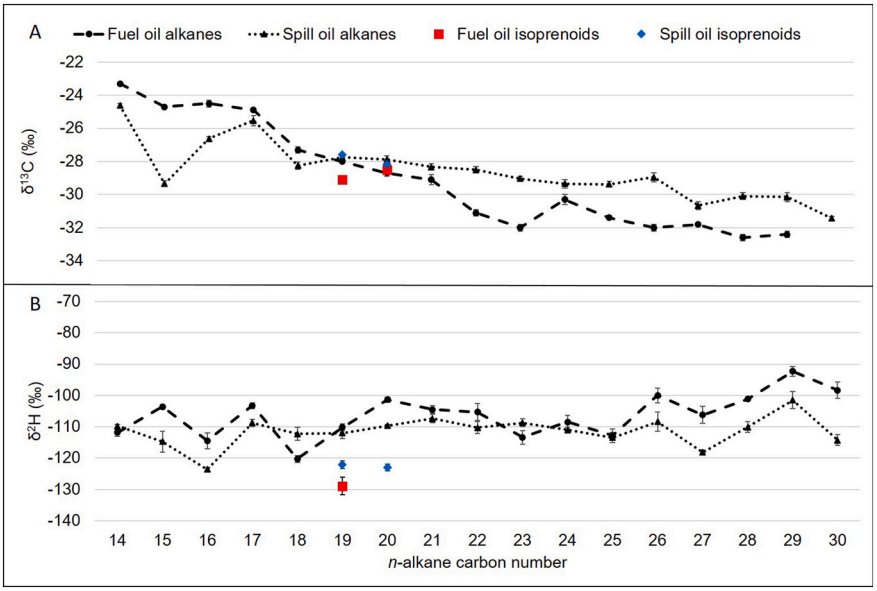

Fig. 7. Stable isotopes ratios (A) $\delta^{13}C$ and (B) $\delta^{2}H$ of *n*-alkanes and isoprenoids pristane (Pr) and phytane (Ph) extracted from Wakashio fuel oil and a sample of spilled oil. Error bars = 1 standard deviation.

rapid dilution and possibly allowed localized concentrations of aromatic compounds sufficiently high to cause some acute toxic effects. Although the potential toxicity arising from aromatic compounds of the spilled oil might be relatively low, the reported high pour point of VLSFOs tends to produce high water-in-oil emulsions which are sticky and persistent (Sørheim et al., 2020), potentially causing harm to marine organisms through physical impact such as clogging of gills or smothering of feathers. Such physical characteristics were beyond the scope of the present study. The variable nature of pour point and other characteristics have been reported in LSFOs (Sørheim et al., 2020) and our preliminary analysis by GC × GC of several low S fuel oils revealed a high degree of diversity in the organic compound profiles (Figs. S10 and S11). A thorough investigation into this variability will be the focus of a subsequent study.

3.8. Conclusions and recommendations

The characterization of the *Wakashio* fuel oil is consistent with that of a VLSFO i.e. total S content ~0.3% and very low concentrations of S-containing heterocyclic compounds. A sample of oily residue collected four NM northwest of where the ship ran aground off the southeast coast of Mauritius was found to possess a hydrocarbon profile that was unlike that of any previously reported spilled oil but matched that of the fuel oil from the *Wakashio*. As such this is, to our knowledge, the first documented major spillage of VLSFO in the environment since the implementation of the IMO regulations. Comparisons of biomarker ratios and profiles of suites of compounds demonstrate that the spilled oil had originated from the *Wakashio* but had undergone a short period of weathering in the warm Mauritius climate resulting in losses of the more volatile and water-soluble components. The weathering was sufficient to alter $\delta^{13}C$ isotopic ratios with values for *n*-alkanes $>n\text{-}C_{20}$ appreciably less negative in the spilled oil compared with the *Wakashio* fuel oil. Elemental analyses of the fuel and spilled oils produced similar values for elements such as vanadium and nickel but suggested that water-oil emulsion had formed following the spill. Unlike some HFO, only low concentrations of high-molecular-weight *n*-alkanes and waxes (above normal GC range) were found to be present in either of the oils.

The potential impact of the spilled oil due to release of toxic PAHs appears to be relatively low compared to traditional marine fuel oils or many crude oils although it is possible that localized concentrations of low molecular weight MAH and PAH could have been sufficient to cause acute toxic effects. Future monitoring of organisms, especially filter-feeding bivalves, should include MAH as these are often overlooked but likely bioaccumulated into organisms and into to the feed web. The comprehensive characterization presented herein, including $\delta^{13}C$ and $\delta^{2}H$ isotopic ratios and elemental data will help with future analyses of beached oil and contaminated organisms in the Mauritius environments. The data will also be useful for comparison with future oil spills involving VLSFO. The class of marine fuels collectively termed VLSFO appear to be highly variable in their organic content so further investigations are required to more fully assess their potential impact on the environment and how best to manage their spillage.

CRediT authorship contribution statement

Alan G Scarlett, Robert K. Nelson, Marthe Monique Gagnon, Christopher M. Reddy, and Kliti Grice conceived the study. Alex I. Holman conducted isotope analyses. Paul A. Sutton conducted high temperature GC analyses. Alan G Scarlett conducted GC–MS. Robert K. Nelson conducted GC × GC–MS analyses. All authors contributed to the writing and editing of the manuscript.

Declaration of competing interest

The authors declare that they have no known competing financial interests or personal relationships that could have appeared to influence the work reported in this paper.

Acknowledgments

We acknowledge those in Mauritius, who wish to remain anonymous, for the timely collection and shipment of the oil residue to Curtin University, Australia. Peter Hopper and Francis Spilsbury (CU) are thanked for technical support. This research did not receive any specific grant from funding agencies in the public, commercial, or not-for-profit sectors. The project at Curtin University was supported by the Australian Research Council (grant numbers LP170101000, LE110100119 and LE130100145. CMR and RKN were supported by the National Science Foundation (OCE-1634478 and OCE-1756242). GC × GC analysis support provided by WHOI's Investment in Science Fund.

Appendix A. Abbreviations used for biomarkers

Compound ID Abbreviation	Compound Name	Mass (Da)
	Isoprenoids	
Pr	Pristane ($C_{19}H_{40}$)	268
Ph	Phytane ($C_{20}H_{42}$)	282
	Diasteranes and steranes	
DiaC27βα-20S	13β,17α(H)20S-diasterane ($C_{27}H_{48}$)	372
DiaC27βα-20R	13β,17α(H)20R-diasterane ($C_{27}H_{48}$)	372
C27αββ-20R	5α,14β,17β,20R-Sterane ($C_{27}H_{48}$)	372
C27αββ-20S	5α,14β,17β,20S-Sterane ($C_{27}H_{48}$)	372
C29ααα-20R	24-ethyl-5α(H),14α(H),17α(H)-20R-cholestane ($C_{29}H_{52}$)	400
C29αββ-20R	24-ethyl-5α(H),14β(H),17β(H)-20R-cholestane ($C_{29}H_{52}$)	400
C29αββ-20S	24-ethyl-5α(H),14β(H),17β(H)-20S-cholestane ($C_{29}H_{52}$)	400
	Hopanoids	
Ts	18α(H)-22,29,30-trisnorneohopane ($C_{27}H_{46}$)	370
Tm	17α(H)-22,29,30-trisnorhopane ($C_{27}H_{46}$)	370
BNH	17α(H),21β(H)-28,30-bisnorhopane ($C_{28}H_{48}$)	384
NH	17α(H),21β(H)-30-norhopane ($C_{29}H_{50}$)	398
C29-Ts	18α(H),21β(H)-30-norneohopane ($C_{29}H_{50}$)	398
NM	17β(H),21α(H)-30-norhopane ($C_{29}H_{50}$) (normoretane)	398
H	17α(H),21β(H)-hopane ($C_{30}H_{52}$)	412
M	17β(H),21α(H)-hopane ($C_{30}H_{52}$) (moretane)	412
HH (S)	17α(H),21β(H)-22S-homohopane ($C_{31}H_{54}$)	426
HH (R)	17α(H),21β(H)-22R-homohopane ($C_{31}H_{54}$)	426
2HH (S)	17α(H),21β(H)-22S-bishomohopane ($C_{32}H_{56}$)	440
2HH (R)	17α(H),21β(H)-22R-bishomohopane ($C_{32}H_{56}$)	440
3HH (S)	17α(H),21β(H)-22S-trishomohopane ($C_{33}H_{58}$)	454
3HH (R)	17α(H),21β(H)-22R-trishomohopane ($C_{33}H_{58}$)	454
4HH (S)	17α(H),21β(H)-22S-tetrakishomohopane ($C_{34}H_{60}$)	468
4HH (R)	17α(H),21β(H)-22R-tetrakishomohopane ($C_{34}H_{60}$)	468
5HH (S)	17α(H),21β(H)-22S-pentakishomohopane ($C_{35}H_{62}$)	482
5HH (R)	17α(H),21β(H)-22R-pentakishomohopane ($C_{35}H_{62}$)	482

Supplementary figures show HTGC-FID chromatograms, a comparison of sterane and diasterane biomarkers plus comparisons for a range of heterocyclic compounds present in *Wakashio* fuel oil and spilled oil. Comparisons of unit mass and exact mass resolutions in 1D chromatograms. 2D chromatograms of several LSFOs are supplied.

Appendix B. Supplementary data

Supplementary data to this article can be found online at https://doi.org/10.1016/j.marpolbul.2021.112917.

References

Asif, M., Fazeelat, T., Grice, K., 2011. Petroleum geochemistry of the Potwar Basin, Pakistan: 1. Oil-oil correlation using biomarkers, delta C-13 and delta D. Org. Geochem. 42, 1226–1240.

Barwise, A.J.G., 1990. Role of nickel and vanadium in petroleum classification. Energy Fuel 4, 647–652.

Booth, A.M., Sutton, P.A., Lewis, C.A., Lewis, A.C., Scarlett, A., Chau, W., Widdows, J., Rowland, S.J., 2007. Unresolved complex mixtures of aromatic hydrocarbons: thousands of overlooked persistent, bioaccumulative, and toxic contaminants in mussels. Environ. Sci. Technol. 41, 457–464.

Booth, A.M., Scarlett, A.G., Lewis, C.A., Belt, S.T., Rowland, S.J., 2008. Unresolved complex mixtures (UCMs) of aromatic hydrocarbons: branched alkyl indanes and branched alkyl tetralins are present in UCMs and accumulated by and toxic to, the mussel Mytilus edulis. Environ. Sci. Technol. 42, 8122–8126.

Chen, H., Nelson, R.K., Swarthout, R.F., Shigenaka, G., de Oliveira, A.H.B., Reddy, C.M., McKenna, A.M., 2018. Detailed compositional characterization of the 2014 Bangladesh furnace oil released into the world's largest mangrove Forest. Energy Fuel 32, 3232–3242.

Dawson, D., Grice, K., Alexander, R., 2005. Effect of maturation on the indigenous δD signatures of individual hydrocarbons in sediments and crude oils from the Perth Basin (Western Australia). Org. Geochem. 36, 95–104. https://doi.org/10.1016/j.orggeochem.2004.06.020. In this issue.

Donkin, P., Widdows, J., Evans, S.V., Brinsley, M.D., 1991. Qsars for the sublethal responses of marine mussels (Mytilus edulis). Sci. Total Environ. 109, 461–476.

Eiserbeck, C., Nelson, R.K., Grice, K., Curiale, J., Reddy, C.M., 2012. Comparison of GC–MS, GC–MRM-MS, and GC×GC to characterise higher plant biomarkers in Tertiary oils and rock extracts. Geochim. Cosmochim. Acta 87, 299–322. https://doi.org/10.1016/j.gca.2012.03.033.

Fingas, M., 2016. Oil Spill Science and Technology, 2nd edition. Gulf Professional Publishing, Cambridge, MA, USA.

Grice, K., Eiserbeck, C., 2014. 12.3 - The analysis and application of biomarkers. In: Holland, H.D., Turekian, K.K. (Eds.), Treatise on Geochemistry, Second edition. Elsevier, Oxford, pp. 47–78.

Hook, S., Batley, G., Ross, A., Holloway, M., Irving, P., 2016. In: Oil Spill Monitoring Handbook. CSIRO Publishing, p. 257. https://ebooks.publish.csiro.au/content/oil-spill-monitoring-handbook.

IMO, 2020. IMO 2020 – cutting sulphur oxide emissions. Available: https://www.imo.org/en/MediaCentre/HotTopics/Pages/Sulphur-2020.aspx. (Accessed 15 March 2021).

Incardona, J.P., Carls, M.G., Teraoka, H., Sloan, C.A., Collier, T.K., Scholz, N.L., 2005. Aryl hydrocarbon receptor-independent toxicity of weathered crude oil during fish development. Environ. Health Perspect. 113, 1755–1762.

Lemkau, K.L., Peacock, E.E., Nelson, R.K., Ventura, G.T., Kovecses, J.L., Reddy, C.M., 2010. The M/V cosco Busan spill: source identification and short-term fate. Mar. Pollut. Bull. 60, 2123–2129.

Lewis, D., 2020. How Mauritius is cleaning up after major oil spill in biodiversity hotspot. Nature 585.

Li, Y., Xiong, Y.Q., Yang, W.Y., Xie, Y.L., Li, S.Y., Sun, Y.G., 2009. Compound-specific stable carbon isotopic composition of petroleum hydrocarbons as a tool for tracing the source of oil spills. Mar. Pollut. Bull. 58, 114–117.

Mitsui-O.S.K.Lines, 2020. Capesize Bulker "Wakashio" Aground off Mauritius (Update 4). Available: https://www.mol.co.jp/en/pr/2020/20045.html. (Accessed 24 November 2020).

Nelson, R.K., Kile, B.M., Plata, D.L., Sylva, S.P., Xu, L., Reddy, C.M., Gaines, R.B., Frysinger, G.S., Reichenbach, S.E., 2006. Tracking the weathering of an oil spill with comprehensive two-dimensional gas chromatography. Environ. Forensic 7, 33–44.

Nelson, J.R., Grubesic, T.H., Sim, L., Rose, K., 2018. A geospatial evaluation of oil spill impact potential on coastal tourism in the Gulf of Mexico. Comput. Environ. Urban. Syst. 68, 26–36.

Nelson, R.K., Gosselin, K.M., Hollander, D.J., Murawski, S.A., Gracia, A., Reddy, C.M., Radovic, J.R., 2019. Exploring the complexity of two iconic crude oil spills in the Gulf of Mexico (Ixtoc I and Deepwater Horizon) using comprehensive two-dimensional gas chromatography (GC x GC). Energy Fuel 33, 3925–3933.

NRC, 2003. In: Oil in the Sea III: Inputs, Fates and Effects. National Research Council (US). National Academies Press, Washington, DC, p. 280.

Peters, K.E., Walters, C.C., Moldowan, J.M., 2005. The biomarker guide: volume 1. In: Biomarkers and Isotopes in the Environment and Human History. Cambridge University Press, Cambridge, England.

Rajendran, S., Vethamony, P., Sadooni, F.N., Al-Kuwari, H.A.-S., Al-Khayat, J.A., Govil, H., Nasir, S., 2021. Sentinel-2 image transformation methods for mapping oil spill - a case study with Wakashio oil spill in the Indian Ocean, off Mauritius. MethodsX 101327.

Ramsar, 2020. Ramsar Sites Information Service. Available: https://rsis.ramsar.org/ris-search/?f%5B0%5D=regionCountry_en_ss%3AAfrica&f%5B1%5D=regionCountry_en_ss%3AMauritius&pagetab=1. (Accessed 24 November 2020).

Scarlett, A., Dissanayake, A., Rowland, S.J., Galloway, T.S., 2009. Behavioral, physiological, and cellular responses following trophic transfer of toxic monoaromatic hydrocarbons. Environ. Toxicol. Chem. 28, 381–387.

Scarlett, A.G., Clough, R., West, C., Lewis, C.A., Booth, A.M., Rowland, S.J., 2011. Alkylnaphthalenes: priority pollutants or minor contributors to the poor health of marine mussels? Environ. Sci. Technol. 45, 6160–6166.

Shimizu, Y., Nakatsuru, Y., Ichinose, M., Takahashi, Y., Kume, H., Mimura, J., Fujii-Kuriyama, Y., Ishikawa, T., 2000. Benzo a pyrene carcinogenicity is lost in mice lacking the aryl hydrocarbon receptor. Proc. Natl. Acad. Sci. U. S. A. 97, 779–782.

Sørheim, K.R., Daling, P.S., Cooper, D., Buist, I., Faksness, L., Altin, D., Pettersen, T., Bakken, O.M., 2020. In: Characterization of Low Sulfur Fuel Oils (LSFO) – A New Generation of Marine Fuel Oils, Trondheim, Norway, p. 112.

Uhler, A.D., Stout, S.A., Douglas, G.S., Healey, E.M., Emsbo-Mattingly, S.D., 2016. 13 - Chemical character of marine heavy fuel oils and lubricants. In: Stout, S.A., Wang, Z. (Eds.), Standard Handbook Oil Spill Environmental Forensics, Second edition. Academic Press, Boston, pp. 641–683.

Wang, Z., Yang, C., Yang, Z., Brown, C.E., Hollebone, B.P., Stout, S.A., 2016. 4 - Petroleum biomarker fingerprinting for oil spill characterization and source identification. In: Stout, S.A., Wang, Z. (Eds.), Standard Handbook Oil Spill Environmental Forensics, Second edition. Academic Press, Boston, pp. 131–254.